Appl. Phys. B 70, 651–655 (2000) / Digital Object Identifier (DOI) 10.1007/s003400000235

Applied Physics B
Lasers
and Optics

Fragmentation of dodecanethiol molecules: application to self-assembled monolayer damage in atom lithography

J.D. Close[1,*], **K.G.H. Baldwin**[1], **K. Hoffmann**[2], **N. Quaas**[2]

[1] Physics Department, The Faculties, and the Research School of Physical Sciences and Engineering, The Australian National University, Canberra, ACT 0200, Australia
[2] Max Planck Institut für Strömungsforschung, Bunsenstrasse 10, 37073 Göttingen, Germany

Received: 20 September 1999/Revised version: 6 December 1999/Published online: 8 March 2000 –

Abstract. Atom lithography commonly employs self-assembled monolayers (SAMs) of alkanethiols which act as resists to protect prepared surfaces. Metastable atomic species such as helium are used to damage the resist, enabling pattern transfer via mask lithography, followed by wet chemical etching. The damage mechanism is, however, not well understood. Here we report studies of fragmentation of dodecanethiol (DDT) molecules embedded in helium nanodroplets that have been irradiated by an electron beam. The results of the charge-transfer fragmentation process provide the first experimental data on the damage mechanisms that occur in the metastable helium/SAM interaction.

PACS: 85.40.Hp; 85.40.Ux; 39.10.+j

Lithography using neutral atomic beams has been successfully employed to create nanoscale structures on specially prepared surfaces [1]. A variety of techniques have been used, including direct deposition of metal atoms [2, 3], as well as the exposure of resist-coated substrates to reactive atomic beams. The latter technique exploits a range of materials for the resists, including physisorbed hydrocarbons which interact with energetic metastable rare-gas atoms to create a protective carbonaceous layer ('contamination' resists [4–8]).

A more common resist employs self-assembled monolayers (SAMs) of hydrocarbons such as alkanethiols and alkylsiloxanes which provide a robust, uniform and extremely thin (few nm) resist layer. The active head group in each case (SH and SiO_x) chemically bonds to an appropriate substrate (gold or SiO_2), with the hydrocarbon chain oriented away from the surface in a regular, self-organized two-dimensional structure. The dangling hydrocarbon chains prevent the deposition of further layers, with the result that damage to a single molecule creates only a very small footprint on the surface. The average molecular density of alkanethiols, for example, is of the order of $5 \times 10^{14}\,\mathrm{cm}^{-2}$ [9–11], implying a footprint of $\approx 0.2\,\mathrm{nm}^2$. This makes SAMs suitable for very high resolution lithography, and exposures using electron beam techniques have yielded features sizes $< 10\,\mathrm{nm}$ [12–15]. In atom lithography, both alkali metal atoms [16–19], and metastable rare gas atoms [20–23] possessing large internal energies (up to 20 eV), have been used to damage SAM-coated substrates.

The unexposed SAM is hydrophobic, whereas the hydrophilic damaged regions are susceptible to wet chemical etching. By coating SAM resists onto metal-coated substrates and damaging the exposed regions through a physical mask, a replica of the mask shape can be patterned into the metal surface by the wet chemical etch. The edge resolution of such techniques is limited mainly by the thickness of the metallic layer, and has been demonstrated to be as small as 30 nm [21], which greatly exceeds the footprint of an individual SAM molecule. Further techniques, such as low-pressure plasma processing [24], can be used to transfer the pattern into the underlying substrate, yielding high (≈ 20) aspect ratio edge structures approaching 1 μm in depth [25].

However, little is known about the interaction between the atoms and the SAMs that causes the damage process. In the case of alkali metal atoms incident on alkanethiol SAMs, one mechanism proposed is the penetration of alkali atoms through open defects in the monolayer, followed by a chemical interaction at the gold–sulphur bond [16].

For metastable atoms, direct physical damage appears to be the more likely mechanism. Rare-gas atoms exist in metastable excited states that have lifetimes ranging from 20 ms to ≈ 8000 s, and which possess internal energies ranging from 8 eV for xenon to 20 eV for helium. This large internal energy exceeds the bond energies in many of the resists employed ($\ll 10$ eV), and may result in bond scission. The more energetic metastable species such as He may also cause Penning ionization. The electron released in the Penning ionization process may result in further damage of adjacent SAM molecules, given that the inelastic electron mean free path is $< 1\,\mathrm{nm}$ in similar materials [26–28]. The higher Penning ionization efficiency of the more energetic (20 eV) metastable He atoms may also explain the order of magnitude lower dosage rates required (≤ 1 monolayer) compared with (12 eV) metastable argon [1].

Figure 1 shows a number of possible bond-breaking processes. In the top sequence, C–H bond breaking results in hydrogen radical abstraction. A radical is also created in the hydrocarbon chain, which may then react with background

*Corresponding author. (E-mail: John.Close@anu.edu.au)

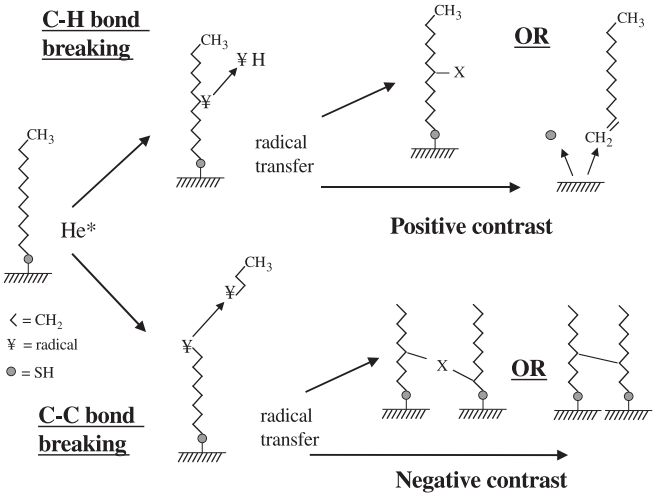

Fig. 1. Possible bond-breaking processes arising from the metastable He/SAM interaction (X denotes background species). The top sequence results in less resistance to wet chemical etching (yielding positive contrast images), whereas the bottom sequence yields a more resistant cross-linked layer

gas constituents (typically oxygen). The appearance of these polar groups enhances the wettability of the SAM and hence its susceptibility to wet chemical etching, resulting in images with positive contrast. Radical transfer along the chain may also result in fragmentation of the molecule at the weaker C–S bond, with subsequent removal of the SAM molecule from the surface altogether.

Alternatively, C–C bond breaking may occur (lower sequence), with the production of carbon chain fragments. Subsequent cross-linking of the dangling bonds may then yield a carbonaceous film with less wettability and hence better resist properties than the original SAM. Consequently, a negative contrast pattern may result following wet chemical etching.

Evidence for cross-linking of the hydrocarbon chains has also been observed in electron beam lithography of SAMs subsequently processed by reactive ion etching (RIE) [15]. These studies show that at low doses, breaking of the C–H bond produces H loss leaving a C-rich film. At much higher doses, further degradation produces fragmentation of the carbon chain, which implies that cross-linking of the fragmented molecules may also be occurring. This results in the formation of a highly resistant carbonaceous layer, as evidenced by the observation of a negative contrast pattern following RIE.

Transitions from positive to negative contrast patterns have been observed for alkanethiol-coated gold surfaces exposed to increasing dosages of metastable He atoms [22]. However, it is not clear from these experiments whether the enhanced resist is due to fragmentation and cross-linking of the SAMs molecules, or is the result of deposition of a precursor film (for example pump oil) which is catalysed by the metastable He atoms in a 'contamination' resist process [1, 4].

The present studies aim to examine more closely the fragmentation of alkanethiol molecules (in particular dodecanethiol or DDT: $CH_3[CH_2]_{11}SH$) in a controlled environment to better understand the origin of the SAMs damage process. We have carried out these studies in a molecular beam. Although the reaction of an isolated molecule may differ from the reaction of the same molecule in a self-assembled monolayer, we have performed this experiment to record the first data on this important system.

1 Experimental concept

An ideal technique for investigating the fragmentation process would be to perform a crossed molecular/atomic beam experiment in which a beam of gas-phase DDT molecules interacts with a beam of metastable He atoms. The products of the dissociation process could then be determined directly using a sensitive mass spectrometer. Unfortunately, metastable He beam fluxes are five orders of magnitude lower than beams of ground state atoms [29]. The low flux, compounded with the low yield obtained from a crossed-beam experiment, makes it extremely difficult, if not impossible, to use this technique.

To overcome these problems, we have opted for a closely related beam experiment providing a readily measurable flux of molecular ion fragments. Here we embed DDT molecules in the diffuse, weakly interacting environment of a superfluid He nano-droplet [30], and fragment the DDT by charge transfer from the He (Fig. 2). The charge-transfer process is initiated by crossing an electron beam with the DDT/He droplets, causing ionization of the He atoms (ionization energy 24.6 eV). Charge transfer within the droplet in turn ionizes and fragments the DDT molecules. The energy released in this process then evaporates the droplet, and enables the remaining DDT ion fragments to be examined in a mass spectrometer.

It is important to compare the similarities and differences between this charge-transfer experiment and the crossed metastable beam experiment. There are two main issues: first, the perturbation of the DDT molecule by the nanodroplet environment, and second, the similarity between the He ion interaction and the metastable He interaction with the DDT molecule.

It is a valid concern that, in the droplet experiment, the surrounding superfluid He may stabilize the embedded molecule against fragmentation or may significantly alter the fragmentation channels. The well-characterized properties of the superfluid He droplet suggest this is not the case. First, the He–He binding energy is three orders of magnitude lower than the binding energy per atom in organic molecules, yielding an essentially non-interacting environment [31]. Second, the superfluid helium is two orders of magnitude lower in density, and forms a very low-density, low-temperature (0.37 K) liquid around the molecule [32]. High-resolution ro-vibrational spectra of organic molecules

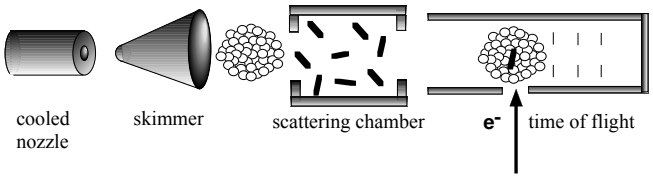

Fig. 2. Schematic diagram of the helium droplet experiment. Helium droplets produced in an expansion of cold helium gas into vacuum are doped with SAMs molecules, ionized, mass selected and detected

embedded in He droplets are well-described by a free rotor Hamiltonian indicating that the molecules rotate and vibrate essentially unhindered in the low-density liquid He droplet [31, 33]. Thus the He environment only weakly perturbs the embedded molecule.

The second difference between our experiment and the metastable He beam experiment is the mechanism leading to the fragmentation. In the droplet experiment, fragmentation of the DDT molecule proceeds via charge transfer from He^+. The production of He^+ in the droplet is an efficient process in which an electron beam of variable energy impacts the droplets, ejecting an electron and producing a positive hole (Fig. 2). The threshold energy for this process is the ionization energy of He (24.6 eV). The positive hole is attracted to the embedded molecule via the ion-induced dipole interaction and ionizes the embedded molecule by charge transfer. As the ionization energy of the molecule (< 10 eV) is much less than the ionization energy of He, this process is always energetically favorable. On transferring the charge, the difference between the ionization energy of He and that of the embedded molecule is released into the droplet. Since the binding energy per He atom is only 0.62 meV, this provides sufficient energy to fragment and evaporate the droplet, allowing mass selection and detection of the isolated DDT molecular ion fragments.

By comparison, in the ideal metastable He experiment, fragmentation proceeds via interaction of the DDT molecule with the excited state He atom, presumably including Penning ionization. The two mechanisms are similar in the important aspect that they both involve highly localized excitations with energies on the order of 20 eV, more than double the ionization energy of the molecule itself. We expect that the fragmentation results from the charge-transfer experiment will yield valuable information on the final products of the DDT/metastable He interaction.

2 Experimental apparatus

The experimental apparatus is similar to that used in other fragmentation measurements in He nanodroplets and is described in detail elsewhere [34]. The superfluid He nanodroplets are produced in a supersonic expansion of cold He gas through a 5-μm-diameter nozzle, into vacuum (Fig. 3). Typical stagnation conditions in the liquid-He-cooled nozzle are 10 K and 20 bar. The average size of the droplets is 20 000 atoms, or 5 nm in radius.

The beam is skimmed and passes through a scattering chamber containing a few ml of liquid DDT at room temperature. The density of DDT vapor in the cell was reduced such that a significant number of droplets collided with, and absorbed, just a single DDT molecule (as measured by the mass spectrometer). The pick-up of foreign molecules by He nano-droplets has been well researched by the group at MPI in Göttingen and others [35–37].

In the following chamber, an electron gun, operating with a beam current of 2 nA and a beam energy that could be varied up to 70 eV, ionized the droplets. The ionization products were analyzed by a reflection time-of-flight mass spectrometer with a mass resolution of approximately 2000.

It is also useful to compare the results of the He/SAM molecule interaction with electron beam lithography on

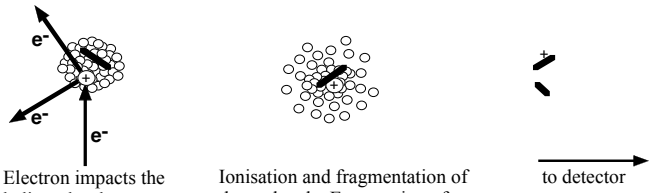

Fig. 3. Principle of the helium droplet fragmentation process. The helium droplet is ionized by electron impact and the embedded molecule is in turn ionized by charge transfer from the helium. Following evaporation of the droplet, the fragmentation products are mass selected and detected in a high-resolution time-of-flight mass spectrometer

SAMs coated surfaces [15]. To this end, a separate experiment was performed using the electron gun to ionize gas-phase (not surrounded by helium) DDT molecules.

3 Results

Figure 4a is the mass spectrum for helium-mediated ionization of DDT embedded in a helium droplet. Figure 4b is the mass spectrum of gas-phase (pure) DDT ionized by direct electron impact. Both spectra were recorded using a 30-eV electron beam. In the droplet experiment, we observed a clear but gradual threshold around 22 eV – 24 eV. The distribution of energies from our electron source makes it impossible to distinguish the threshold at 20 eV, corresponding to the production of metastables, from that at 24.6 eV corresponding to ionization of the droplet. As ionization of the droplet is more efficient, we have assumed this is the dominant process [36]. Above 20 eV, the measured mass spectrum was found to be independent of electron beam energy. We observed no signal for electron impact energies below 20 eV in stark contrast to our results on a free beam of DDT, clearly indicating that our entire signal in the droplet experiment is due to ionization mediated by helium.

The gas-phase spectrum, measured using direct impact ionization of a pure DDT molecular beam, was found to be independent of electron energy for energies between 10 eV and 70 eV. Here, we observed a clear but gradual threshold in the

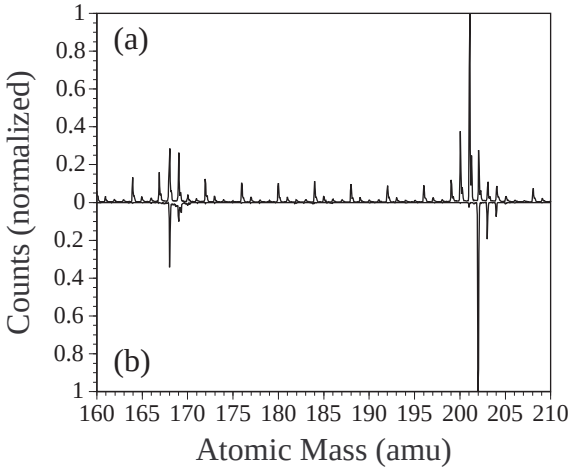

Fig. 4. Mass spectrometer signal as a function of mass number for (a) the helium-droplet experiment and (b) the gas-phase experiment

signal around 10 eV corresponding to the ionization energy of the molecule.

In the gas phase experiment (Fig. 4b), the region studied includes the range from the mass peak of a complete DDT molecule (202 amu) to the region in which the loss of up to four CH_2 (14 amu) fragments and SH (33 amu) fragmentation can be detected. The major features of the spectrum occur around peaks at 202 and 169 amu. The main peak at 202 amu is the molecular ion, whereas the peak at 203 amu is the molecular ion with a single ^{13}C in the carbon chain. The ratio of these two peaks is 9 : 1, consistent with the natural abundance of ^{13}C (1.1%) and the length of the carbon chain. The major contribution (90%) of the peak at 204 amu is due to the presence of the ^{34}S isotope, occurring with a natural abundance of 4.4%. The remaining 10% of this peak comes from the molecular ion with two ^{13}C atoms in the carbon chain. The small peak at 201 amu is the molecular ion at 202 amu less the alpha hydrogen. This is a well-known fragmentation channel in mass spectra recorded using electron impact [38].

The peak at 168 amu is the main feature in this part of the gas-phase mass spectrum and corresponds to the molecular ion less either $^{32}SH_2$ or the corresponding ion less $^{34}SH_2$. The peak at 169 amu is mainly due to the loss of ^{32}SH. Small contributions also come from the loss of $^{32}SH_2$ from the molecular ion responsible for the peak at 203 amu, and a yet smaller contribution from the loss of $^{34}SH_2$ from the peak at 204 amu. The small peak at 170 amu arises from the loss of ^{32}SH from the peak at 203 amu with a contribution from the peak at 204 amu less $^{34}SH_2$. Apart from the small peak at 201 amu, there is no evidence for the removal of more than a single hydrogen atom along the chain in the gas-phase experiment.

In the droplet experiment (Fig. 4a), the series of small peaks occurring at multiples of 4 amu are due to ionized He droplets. This background must be subtracted from all peaks occurring at multiples of 4 amu. The peaks at 168, 169, 170, 201, 202, 203, and 204 amu have the same origin as those observed in the gas phase. The dominant peak in this case, however, is the molecular ion *less* one hydrogen. There are also strong peaks at 199 and 200 amu corresponding to the loss of hydrogen atoms along the carbon chain. These peaks are not observed in the gas-phase spectrum. A new peak also occurs at 167 amu, corresponding to the loss of $^{32}SH_2$ and one more hydrogen atom along the carbon chain. The absence of subsidiary peaks at 14-amu intervals indicates that there is no evidence for the loss of C-containing fragments in either spectrum.

The following summarizes the results of these experiments.

1. Electron beam interactions with the gas-phase DDT resulted in single C–H bond-breaking
2. Both single and multiple C–H bond-breaking occur in the charge-transfer (droplet) process
3. In both processes breaking of the C–S bond occurs
4. In neither case is there evidence for breaking of the C–C bond.

4 Conclusion

These fragmentation results have potential implications for the interaction of metastable helium atoms with SAMs coated substrates. The damage processes identified here (breaking of the C–H and C–S) bonds will increase the polar nature of the surface and create nano-defects, which in turn will increase the wettability of the surface and enhance the penetration of wet chemical etchants. This is consistent with experiments involving the exposure of DDT SAMs to low (≤ 1 monolayer) dosages of metastable atoms, where positive contrast images have been created following wet chemical etching.

The results presented here can also be compared with studies of SAMs damage processes using electron beam lithography [15]. The electron beam experiments show evidence for C–H bond-breaking at low fluxes, which results in positive contrast patterns from wet chemical etching. At higher fluxes substantial C loss occurs, and a negative contrast pattern is produced for reactive ion etching, indicating that a more resistant layer is produced in the exposed regions. This implies that extensive cross-linking of the hydrocarbon chains occurs at high doses, caused by the widespread breaking of C–C bonds which then re-form between adjacent damaged molecules.

In the present experiments we see no evidence for C–C bond-breaking. This suggests that the negative contrast images observed in metastable He exposures to DDT SAMs may not be caused by cross-linking of the DDT molecules themselves. The negative contrast images that have been observed might alternatively have resulted from the interaction of metastable He atoms with contaminants on the substrate (such as pump oil), that are then cross-linked to form more effective resists than the original SAM layer.

Acknowledgements. We would like to acknowledge the assistance of Frank Federmann and the hospitality of Professor J.P. Toennies of the Max Planck Institut für Strömungsforschung. We thank J. MacLeod (ANU) for some enlightening discussions and Tim Senden (ANU) for helpful suggestions and his reading of the manuscript.

References

1. For a review see J.H. Thywissen, K.S. Johnson, R. Younkin, D.H. Dekker, K.K. Berggren, A.P. Chu, M. Prentiss: J. Vac. Sci. Technol. B **15**, 2093 (1997)
2. G. Timp, R.E. Behringer, D.H. Tennant, J.E. Cunningham, M. Prentiss, K.K. Berggren: Phys. Rev. Lett. **69**, 1636 (1992)
3. J.J. McClelland, R.E. Scholten, E.C. Palm, R.J. Celotta: Science **262**, 877 (1993)
4. K.S. Johnson, K.K. Berggren, A. Black, C.T. Black, A.P. Chu, N.H. Dekker, D.C. Ralph, J.H. Thywissen, R. Younkin, M. Tinkham, M. Prentiss, G.M. Whitesides: Appl. Phys. Lett. **69**, 2273 (1996)
5. S.J. Rehse, A.D. Glueck, S.A. Lee, A.B. Goulakov, C.S. Menoni, D.C. Ralph, K.S. Johnson, M. Prentiss: Appl. Phys. Lett. **71**, 1427 (1997)
6. J.H. Thywissen, K.S. Johnson, D.H. Dekker, M. Prentiss, S.S. Wong, K. Weiss, M. Grunze: J. Vac. Sci. Technol. B **16**, 1155 (1998)
7. K.S. Johnson, J.H. Thywissen, N.H. Dekker, K.K. Berggren, A.P. Chu, R. Younkin, M. Prentiss: Science **280**, 1583 (1998)
8. J.H. Thywissen, K.S. Johnson, N.H. Dekker, A.P. Chu, M. Prentiss: J. Vac. Sci. Technol. **16**(6), 3841 (1998)
9. C.E.D. Chidsey, G.-Y. Liu, P. Rowntree, G.J. Scoles: J. Chem. Phys. **91**, 4421 (1989)
10. N. Camillone III, P. Eisenberger, T.Y.B. Leung, P. Swartz, G. Scoles, G.E. Poirier, M.J. Tarlov: J. Chem. Phys. **101**, 11031 (1994)
11. G.E. Poirier, M.J. Tarlov, H.E. Rushmeier: Langmuir **10**, 3383 (1994)
12. M.J. Lercel, R.C. Tiberio, P.F. Chapman, H.G. Craighead, C.W. Sheen, A.N. Parikh, D.L. Allara: J. Vac. Sci. Technol. B **11**, 2823 (1993)

13. R.C. Tiberio, H.G. Craighead, M. Lercel, T. Lau, C.W. Sheen, D.L. Allara: Appl. Phys. Lett. **62**, 476 (1993)
14. M.J. Lercel, H.G. Craighead, A.N. Parikh, K. Seshadri, D.L. Allara: Appl. Phys. Lett. **68**, 1504 (1996)
15. K. Seshadri, K. Froyd, A.N. Parikh, D.L. Allara, M.J. Lercel, H.G. Craighead: J. Phys. Chem. **100**(39), 15, 900 (1996)
16. M. Kreis, F. Lison, D. Haubrich, D. Meschede, S. Nowak, T. Pfau, J. Mlynek: Appl. Phys. B **63**, 649 (1996)
17. F. Lison, H.-J. Adams, D. Haubrich, M. Kreis, S. Nowak, D. Meschede: Appl. Phys. B **65**, 419 (1997)
18. K.K. Berggren, R. Younkin, E. Cheung, M. Prentiss, A.J. Black, G.M. Whitesides, D.C. Ralph, C.T. Black, M. Tinkham: Adv. Mater. **9**, 52 (1997)
19. R. Younkin, K.K. Berggren, K.S. Johnson, M. Prentiss, D.C. Ralph, G.M. Whitesides: Appl. Phys. Lett. **71**, 1261 (1997)
20. K.K. Berggren, A. Bard, J.L. Wilbur, J.D. Gillaspy, A.G. Helg, J.J. McClelland, S.L. Rolston, W.D. Phillips, M. Prentiss, G.M. Whitesides: Science **269**, 1255 (1995)
21. S. Nowak, T. Pfau, J. Mlynek: Appl. Phys. B **63**, 203 (1996)
22. K.G.H. Baldwin, W. Lu, D. Milic, R.M.S. Knops, M.D. Hoogerland, S.J. Buckman: Proc. SPIE **2995**, 11 (1997)
23. A. Bard, K.K. Berggren, J.L. Wilbur, J.D. Gillaspy, S.L. Rolston, J.J. McClelland, W.D. Phillips, M. Prentiss, G.M. Whitesides: J. Vac. Sci. Technol. B **15**, 1805 (1997)
24. A.J. Perry, R.W. Boswell: Appl. Phys. Lett. **55**, 148 (1989); A.J. Perry, D. Vender, R.W. Boswell: J. Vac. Sci. Technol. B **9**, 310 (1991)
25. W. Lu, K.G.H. Baldwin, M.D. Hoogerland, S.J. Buckman, T.J. Senden, T.E. Sheridan, R.W. Boswell: J. Vac. Sci. Technol. **16**(6), 3846 (1998)
26. M.P. Seah, W.A. Dench: Surf. Interface Anal. **1**, 2 (1979)
27. Y. Harada, S. Yamamoto, M. Aoki, S. Masuda, T. Ichinokawa, M. Kato, Y. Sakai: Nature **372**, 657 (1994)
28. D.M. Oro, P.A. Soletsky, X. Zhang, F.B. Dunning, G.K. Walters: Phys. Rev. A **49**, 4703 (1994)
29. M.D. Hoogerland, D. Milic, W. Lu, H.-A. Bachor, K.G.H. Baldwin, S.J. Buckman: Aust. J. Phys. **49**, 567 (1996)
30. S. Grebenev, J.P. Toennies, A.F. Vilesov: Science 2083, **279** (1998)
31. M. Hartmann, R.E. Miller, J.P. Toennies, A.F. Vilesov: Science **272**, 1631 (1996)
32. M. Hartmann, R.E. Miller, J.P. Toennies, A. Vilesov: Phys. Rev. Lett. **75**, 1566 (1995)
33. M. Hartmann, F. Mielke, J.P. Toennies, A.F. Vilesov, G. Benedek: Phys. Rev. Lett. **76**, 4560 (1996)
34. A. Bartelt, J.D. Close, F. Federmann, N. Quaas, J.P. Toennies: Phys. Rev. Lett. **77**, 3525 (1996)
35. A. Scheidemann, J.P. Toennies, J. Northby: Phys. Rev. Lett. **64**, 1899 (1990)
36. M. Lewerenz, B. Schilling, J.P. Toennies: J. Chem. Phys. **102**, 8191 (1995)
37. S. Goyal, D.L. Schutt, G. Scoles: Phys. Rev. Lett. **69**, 933 (1992); F. Stienkemeyer, W.E. Ernst, J. Higgins, G. Scoles: J. Chem. Phys. **102**, 615 (1995)
38. E.J. Levy, W.A. Stahl: Anal. Chem. **33**, 707 (1961)